Contents lists available at Mapta Publishing Group

Vol. 1, No. 2, August, 2018

Mapta Journal of Electrical and Computer Engineering (MJECE)

journal homepage: http://maptapublishing.com/index.php/mjece

ISSN: 2631-5718

Fault Location in Distribution Network Based on Fault Current Analysis Using Artificial Neural Network

Masoud Dashtdar*

Electrical Engineering Department, Faculty of Engineering, Islamic Azad University, Bushehr, Iran

Article Info

Article history:

Received May 18th, 2018
Revised Jul 25th, 2018
Accepted Aug 5th, 2018

Keyword:

Fault location
Wavelet transform
ANN
WEE
EPU

Abstract

In this study, fault location is implemented on an IEEE-15bus sample network using artificial neural network. The basis of this work is such that initially, in order to train the neural network, a series of specific characteristic are extracted by the relay from the observed fault signal. These characteristics are obtained by wavelet transform which properly extracts high and low frequency coefficients of the signal. Hence, since high frequencies are generated during the occurrence of the fault, signal information could be extracted using wavelet transform. After wavelet transform, the entropies of the minor components of the sequences could be obtained using statistics to extract the hidden features inside them and present them to train the neural network. Also, since the obtained inputs for the training of the neural network depend on the fault angle, resistance and location, the training data should be selected such that these differences be properly presented so the neural network does not face any issues in its identification. Therefore, selecting the signal processing function, data spectrum and subsequently, statistical parameters and their combinations are important. The simulation results show the good performance of neural network for the faults in different angles, locations, and resistances.

1. Introduction

Fault identification is one of the most interesting and significant topics for electrical engineers. At the beginning, most researches started focusing on fault location in transmission lines due to the impact of transmission line faults in power systems as well as high required time for the physical investigation of the lines. However, due to being in a reconstructed environment and the rivalry of corporations to increase the access of the users to energy, more attention is paid to the faults of distribution systems. In general, fault location methods could be categorized into three classes including impedance and main frequency components based methods [1-8], high frequency and mobile waves based methods [9-17], knowledge and cognition based methods [18-25]. In the first type of methods, the impedance could be computed up to the fault point by voltage and current measurement in the fault terminal. These types of method are utilized more due to their convenience. However, in distribution lines, multiple faults locations could be obtained due to the presence of multiple branches and having the information only at the beginning of the feeder. In the second types of methods, the basis is on the reflection and transmission of the generated mobile waves at the fault point. Although location could be carried out with high accuracy, implementing these methods is more complex and expensive compared to the impedance based methods. This is due to the fact that these method need several auxiliary equipment such as unsteady fault detector systems, detection and identification software and measurement devices with very high sampling frequencies (MHz). Third type of methods are knowledge based. These methods could be classified into three sub-groups including artificial intelligence, analysis and statistics based methods, distribution device based methods and hybrid methods. One of methods is using artificial neural network based algorithms which act based on learning algorithms. In case of proper implementation, learning based strategies can show acceptable flexibility and performance in different conditions despite certainties in the system. Also, extracting the efficient features and implementing a proper learning

* Corresponding author: dashtdar.masoud@gmail.com

algorithm are two major and effective topics in establishing learning based methods. Therefore, one should extract certain features from the fault signal which reflects the fault situation.

In [26, 27], ANNs (Artificial Neural Networks), and similarly in [28], an ANN and wavelet analysis based method, and in [29] a method based on irregular sets and ANN are presented for fault location in transmission lines. In [30], have used an adaptive network based fuzzy inference system. Nevertheless, devised method for transmission networks are prone to errors due to non-similarity with distribution networks. In [31], fault section identification and fault location are presented in distribution network using artificial neural networks which shows acceptable performance for low resistances. However, in high resistances, the neural network has face issues in its identification.

In this study, two neural networks are used for fault section identification and fault location. One of these networks is used for section identification and the other one is used for estimating the distance. The input training data are identical for both networks. But, the outputs of the two networks are not the same. Also, the training data are obtained by a series of processes. In fact, by applying wavelet transform on the detected fault current by the relay and calculating its entropy, one could generate the training data. The simulation results show that unlike [31], one could design the neural network such that it shows good performance for resistances up to 100 Ohm as well. In the second section, the proposed wavelet transform and neural network based method is described and in the third section, the implementation of the network and the fault location algorithm are presented. In the fourth section, the results of this approach are presented and finally, the conclusion is made in section five.

2. The proposed method

This study is based on neural network learning to enable us to estimate the fault section, the distance from the fault location, and fault resistance in the distribution network. In order to make the fault in the distribution network understandable to the neural network, one should extract a series of distinguishable features from the fault signal observed by the relay and provide it for the neural network for training. As it is known, high frequency waves are generated at the time of the occurrence of the fault. Therefore, by extracting the high frequency components, one could obtain certain features of the fault signal. One method to extract these components is using wavelet transform.

2.1. Wavelet transform

Wavelet transform is able to display signals using a region windowing technique with different sizes such that it enables using large and small temporal windows when accurate information are needed at low frequencies and high frequencies, respectively. One of the major advancements due to wavelet transform is the signal local analysis capability which enables the analysis of a small region of extensive signals. In fact, wavelet is a wave form with limited time period with zero effective value. Wavelets are irregular and asymmetric and their energy is concentrated, limited and is around one point. Wavelet transform consists of breaking a signal to transferred signals and scaling of the main wavelet signal (mother wavelet). Therefore, signal variations analysis using wavelets is better than Fourier analysis with sinusoidal waves and one could conclude that the local variations are better done with wavelets.

Wavelet transform possesses a characteristic called mother wavelet with different types. This transform separates the wave similar to the mother wavelet among all of the available waves and then arranges the separated wave based on the types of high and low frequency components such that the initial wave could be obtained by superimposing them. As a sample, in figure 1 the separation of the waves which consist the fault signal observed by the relay is depicted using wavelet transform. As it could be seen, two approximate and minor components are acquired for each level which are associated with low and high frequency information of the signal, respectively. Therefore, one could reveal the hidden fault information using wavelet transform and since high frequency waves are generated at the time of the fault, our focus is mostly on the minor components. Also, the higher the decomposition levels, the more accurate the results. However, in this study, the focus is mostly on the level 5 minor components.

Wavelet transform is a linear transform which maintains the temporal allocation in different frequency components in the given signal. Therefore, considering a scale function φ and a wavelet function ψ, one could write (1) and (2):

$$\varphi(x) = \sum_k h(k)\sqrt{2}\varphi(2x-k) \quad (1)$$

$$\psi(x) = \sqrt{2}\sum_k (-1)k h(-k+1)\varphi(2x-k) \quad (2)$$

Where h(k) coefficient are calculated as follows (3):

$$h(k) = \varphi(x), \varphi(2x-k) > \quad (3)$$

Thus, one could express a family of function as a linear composition of scale (4) and wavelet functions (5) with shifts and delays:

$$\varphi_{j,k}(x) = 2^{j/2}\varphi(2^j x - k) \quad (4)$$

$$\psi_{j,k}(x) = 2^{j/2}\psi(2^j x - k) \quad (5)$$

Usually, the space expressed by φj,k and ψj,k with shift k are designed with Vj and Wj, respectively such that (6) and (7):

$$V_o \subset \cdots \subset V_j \subset \cdots L^2 \quad (6)$$

$$V_{j+1} = V_j \oplus W_j \quad (7)$$

Each function b(x) ∈ L2 could be expressed in the form of a linear composition of the scale and wavelet functions (8) which are defined by (4) and (5).

$$f(x) = \sum_k C_{j,k}\varphi_{j,k} + \sum_j \sum_k \omega_{j,k}\psi_{j,k} \quad (8)$$

Where

$$C_{j,k} = f(x), \varphi_{j,k} >$$
$$\omega_{j,k} = f(x), \varphi_{j,k} > \quad (9)$$

Therefore, according to figure 1 one could write:

$$f(x) = A1 + D1 = (A2 + D2) + D1$$
$$\big((A3 + D3) + D2\big) + D1$$
$$\Big(\big((A4 + D4) + D3\big) + D2\Big) + D1 \quad (10)$$
$$\Big(\Big(\big((A5 + D5) + D4\big) + D3\Big) + D2\Big) + D1$$

In discrete wavelet transform, a couple of high-pass and low-pass filters are applied to the main function and its derivations. This will result in approximations of the main function and each provides more information regarding the main function in its specific minor scale. The first scale covers a wide frequency bandwidth at the end of the main signal frequency spectrum and higher scales entail lower frequencies with lower bandwidth. The first scale has the highest temporal resolution. However, higher scales have higher incremental temporal periods. In this study, Daubechies wavelet function (db2) is used as the mother wavelet in all transformations.

2.2. Wavelet energy entropy

At the time of the occurrence of the faults, signals containing transients and harmonics are generated. For the sake of proper use of these information, one could extract certain features from the fault signal. One of the methods is using wavelet energy entropy (same as [31]) for the calculation of the energy of the detail components since these components contain high frequency information. Wavelet Energy Entropy (WEE) is evolved by [32-34] which is able to illustrate the energy information in the signal or the system. Wavelet energy of a signal in scale j and instant k is calculated as follows (11):

$$E_{jk} = \left| D_j(k) \right|^2 \quad (11)$$

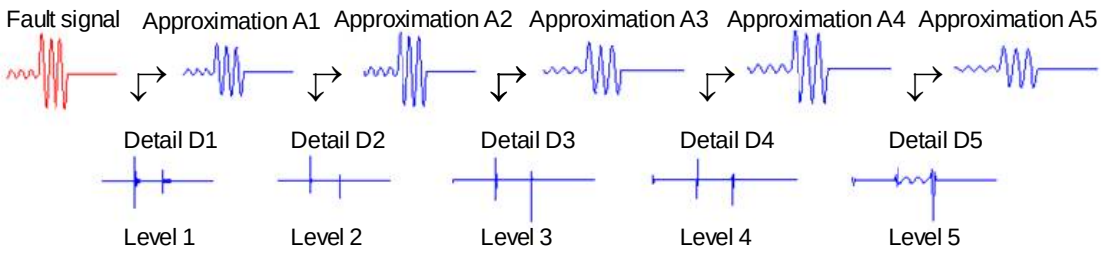

Figure 1. 5-level fault signal decomposition.

In the j-th scale with k = 1, 2, 3,. . ., N, N is the number of instants (coefficient) in the j-th scale and L is the number of decomposition levels. The energy spectrum of the wavelet of the signal in the j-th scale is as follows (12):

$$E_j = \sum_{k=1}^{N} E_{jk} , j = 1^{'}, L \tag{12}$$

The relative wavelet energy in [33] is as follows which shows the energy distribution (13):

$$P_{jk} = \frac{E_{jk}}{E_j} , j = 1^{'}, L \tag{13}$$

Therefore, the WEE (14) is as follows:

$$WEE_{jp} = -\sum_k P_{jkp} log P_{jkp} , j = 1^{'}, L \tag{14}$$

Also, the wavelet entropy index of each unit (15) is obtained as the equation below:

$$EPU_{jp} = \frac{WEE_{jp}}{(WEE_{jA}) + (WEE_{jB}) + (WEE_{jC})} \tag{15}$$

Where, p ∈ {A, B, C} is the phases of the distribution network (15) is the basis for the selection and extraction process. The extracted features are used as the input for trained ANN models for the identification of the fault section and fault point location. Also:

$$EPU_A + EPU_B + EPU_C = 1 \tag{16}$$

2.3. Modeling Artificial Neural Network (ANN)

In this study, similar to [31], two neural networks are used for fault identification and location. The difference is that the training data are selected more purposefully and the structure of the neural network as well as the transfer functions of its hidden layers are different as well. In the primary neural network, the inputs are the calculated phase entropies and its output is the fault section which consists of four outputs in 0 and 1 binaries. These binary numbers introduce the sections as the sections are introduced in the neural network in binaries. The input of the secondary neural network is the same as the primary neural network. However, it has two outputs i.e. fault distance and fault resistance which unlike [31], the impact of the resistance is considered at the output which will be pointed out in the following paragraphs. Both neural networks are consisted of two hidden layers. In the primary network, transfer functions tansig(n) and tansig(n) and in the secondary network, functions logsig(n) and purelin(n) are used in the hidden layers. Transfer function are used for determining the characteristics of the neuron for solving different problems. In figure 2 the structure of these function are illustrated. Also, traingdx and trangdm training functions are used in the primary and secondary networks, respectively.

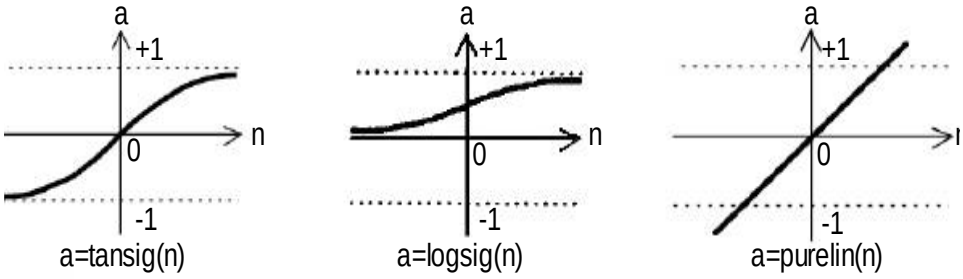

Figure 2. The transferred function used in the primary and secondary neural network.

2.3.1. Primary neural network (ANN-Primary)

As pointed out, primary neural networks are used for the identification of the fault section. Since the faults occur in different types, the primary neural network should be trained depending on the type of the fault. It means that it identifies the fault section for single-phase, two-phase, two-phase-to-ground or three-phase faults. In figure 3 the structure of the primary neural network is depicted. In this network, in addition to entropy phases, positive and zero sequence energies are considered as the input. It is known that positive sequence energy exists for all of the faults and zero sequence has the maximum values for the earth faults. Therefore, it is a good criterion for fault identification. This network output is a series of binary numbers.

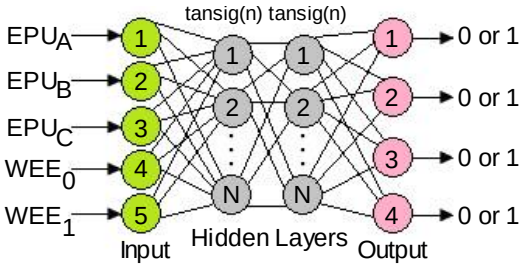

Figure 3. The structure of the primary neural network for the identification of the fault section.

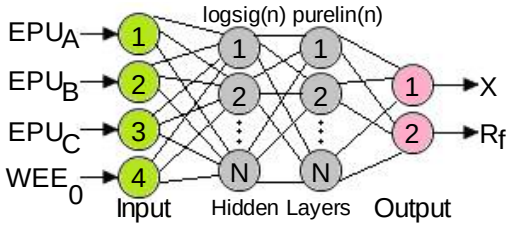

Figure 4. The Structure of secondary neural network to estimate the distance and fault resistance.

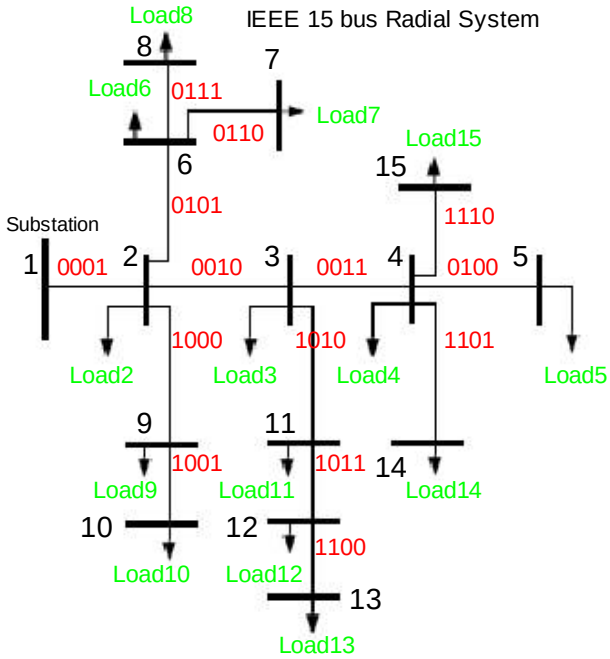

Figure 5. The sample network.

2.3.2. Secondary neural network (ANN-Secondary)

Secondary neural network can be used to estimate the distance from the fault location and also to obtain the fault resistance. The reason for considering the resistance at the output of the network is that in [31], the presented algorithm has acceptable accuracy for low resistances. However, it faces issues for high resistances. The studies show that the calculated entropy strongly depends on the fault angle and fault resistance. Therefore, one could highly improve the accuracy of the algorithm by considering these parameters in the output of the neural network. The results of the study properly reflect the performance of the proposed algorithm. In figure 4 the structure of the secondary neural network is depicted. The outputs of this network are the fault distance and resistance.

3. Network implementation

The proposed method is implemented on a standard radial IEEE_15bus network. The radial network IEEE_15bus has a rated voltage of 11 kV and total feeder load 1226.4 kW and 1251.11kvar. Figure 5 shows the radial network

IEEE_15bus being studied. As seen in figure 5 each section is named by binaries to be definable for the neural network. Also, the length of each section is considered to be 10 km and all of the simulations are carried out using MATLAB software. In table 1, the information regarding the neural network is presented.

4. Simulation results

First, to extract and generate training data, each network line of figure 5 is studied for the conditions of occurrence of different types of faults. The results of the study show that the obtained entropies are different for each line and have strong dependence on the fault occurrence angle, fault resistance, and type of the fault. Considering the limitations of the pages of the paper, the results of the studies on sections 0010 and 1110 are briefly presented.

In the figures following, all the red lines with different symbol depict the entropy of the phase of the fault. Figure 6 to figure 11 show the entropy variations for resistances 0.5 to 100 Ohm in fault distance 500 meters from the line and figure 12 to figure 15 show the entropy variations for fault distances of 0.5 to 9 kilometers. Also, at the time of the occurrence of the fault, phase angles a, b, and c are 160, 40, and -80 degrees, respectively. In [31], it is pointed out that the value of the entropy of the phase of fault is less than the entropy of the phases without faults. However, the results of the studies properly show that this is not always true and it is possible that the minimum value exists only in certain ranges. As seen from the results, the value of the entropies strongly depend on the fault phase, angle of the fault occurrence, and the value of the resistance such that in single-phase faults, the variations of the entropy of the fault phase are symmetric with respect to the other two phases and in two-phase faults, the values of the entropy of the two phases are symmetric as well. But, these two phases do not necessarily contain faults. In figure 16 the variations of the area under the current curve are illustrated for the conditions of the occurrence of the fault for different angles. According to figure 16 it seems that the calculated entropy should be the maximum for angle 160 degrees. However, this is not always true since the fault distance and resistance could lead to a decrease in the fault phase entropy.

Table 1. Parameters of the primary and secondary neural network.

ANN- Secondary	ANN- Primary	Parameters
4	5	Input
2	4	Output
traingdm	Traingdx	Training algorithm function
logsig(n)	tansig(n)	Hidden layer1 function
purelin(n)	tansig(n)	Hidden layer2 function
Batch-mode	Batch-mode	Weight update method

Table 2. Information of the effective parameters on the fault for generating the training entropies

Parameters effective on fault						
Fault location (km)	Fault resistance (ohm)	Fault inception angle (Degree)	Fault type			
			1 Ph.g	2 Ph.g	2 Ph	3 Ph
0.5	0.5	160	A-g	A-B-g	A-B	A-B-C
3	20	40	B-g	A-C-g	A-C	
6	40	-80	C-g	B-C-g	B-C	
9	60					
	80					
	100					

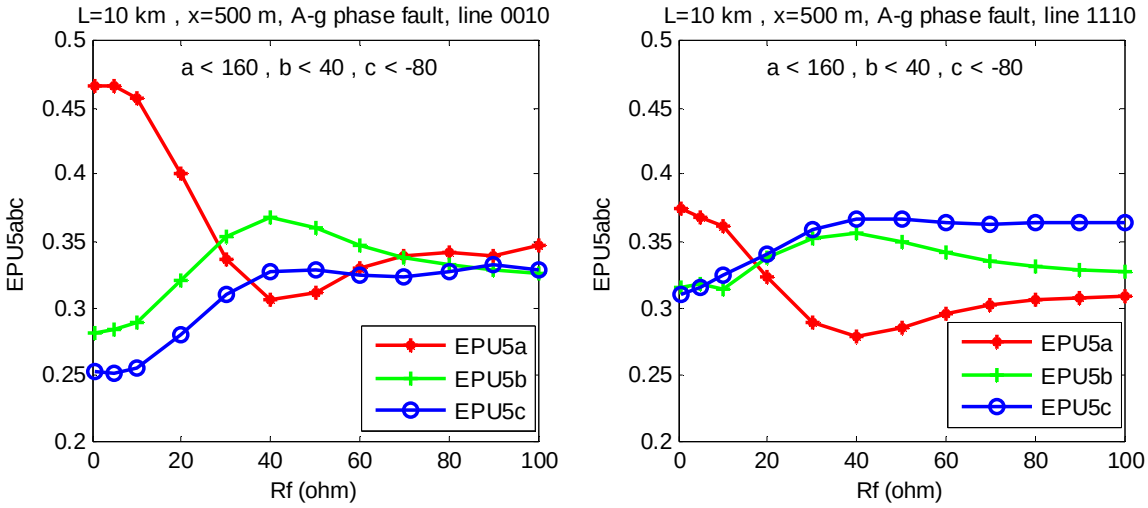

Figure 6. A-g single-phase-to-ground fault.

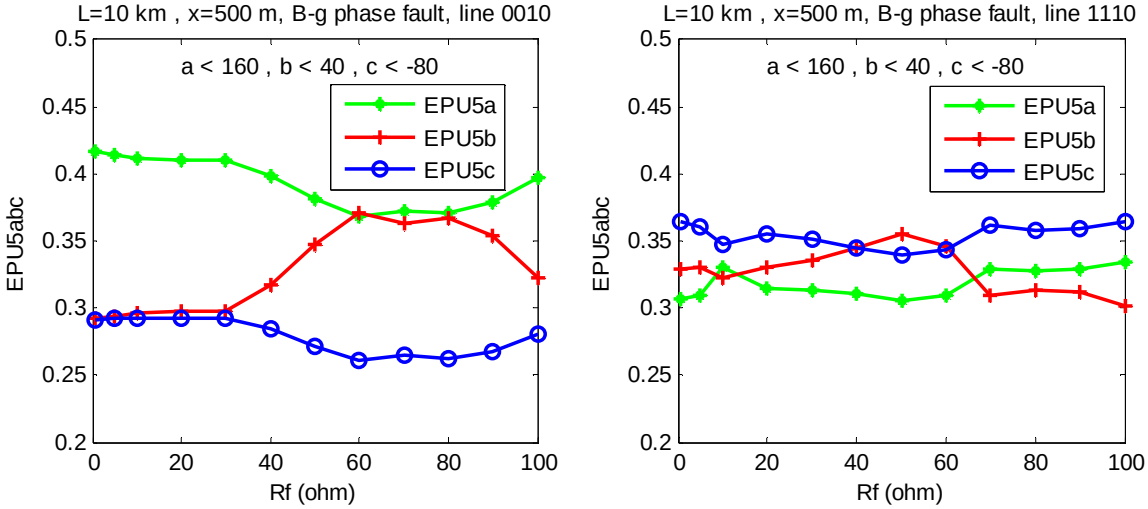

Figure 7. B-g single-phase-to-ground fault.

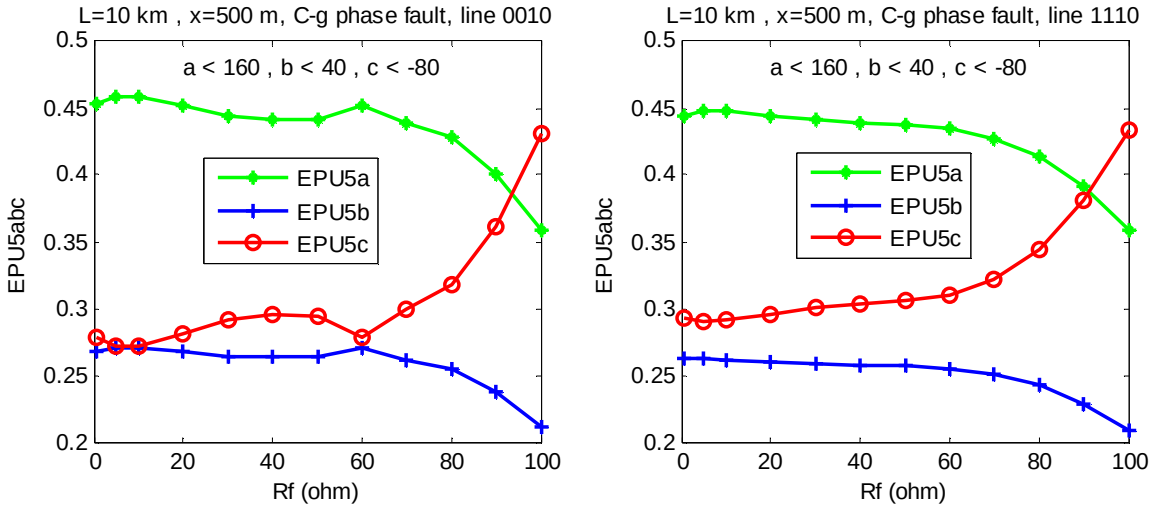

Figure 8. C-g single-phase-to-ground fault.

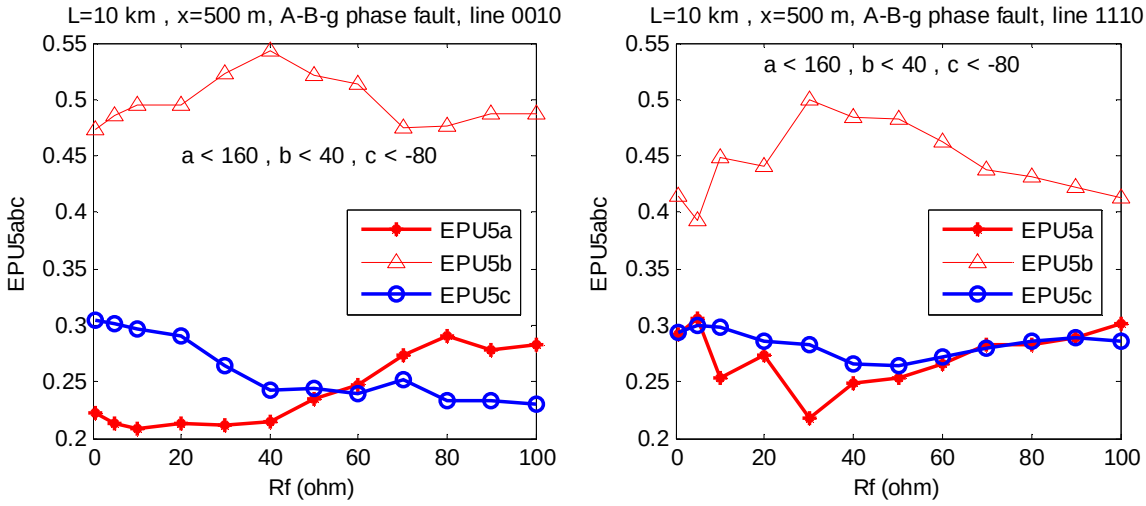

Figure 9. A-B-g two-phase-to-ground fault.

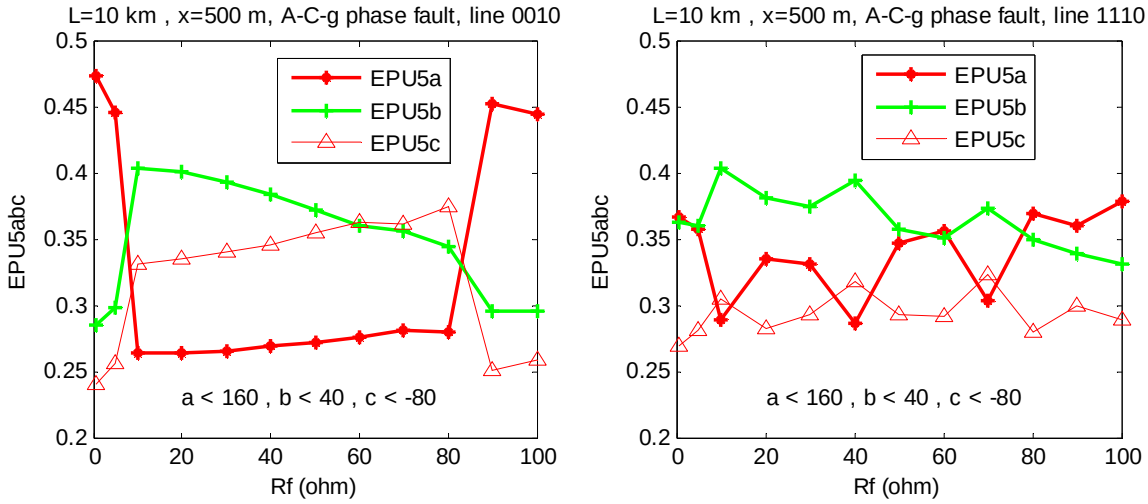

Figure 10. A-C-g two-phase-to-ground fault.

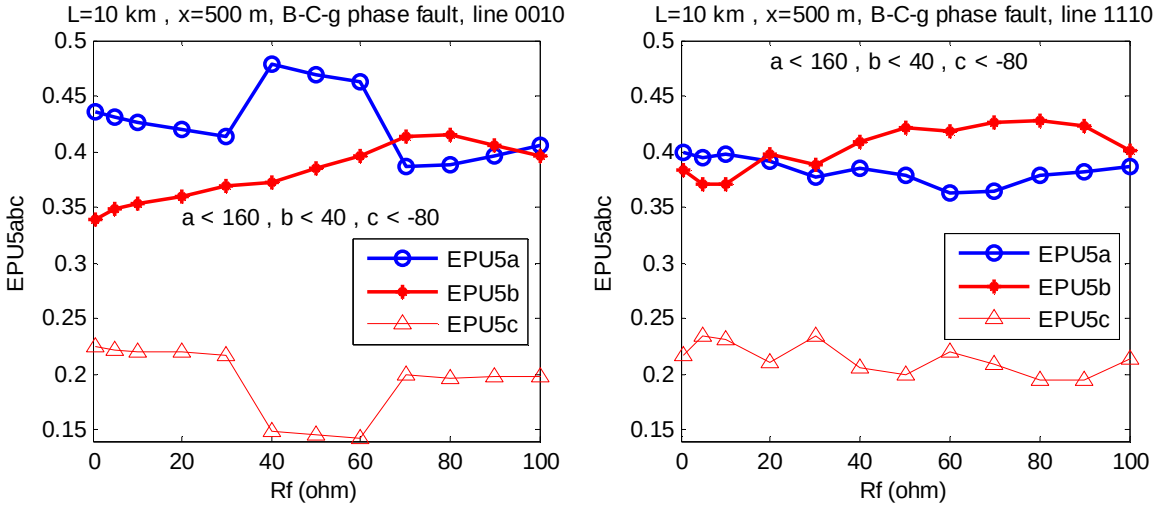

Figure 11. B-C-g two-phase-to-ground fault.

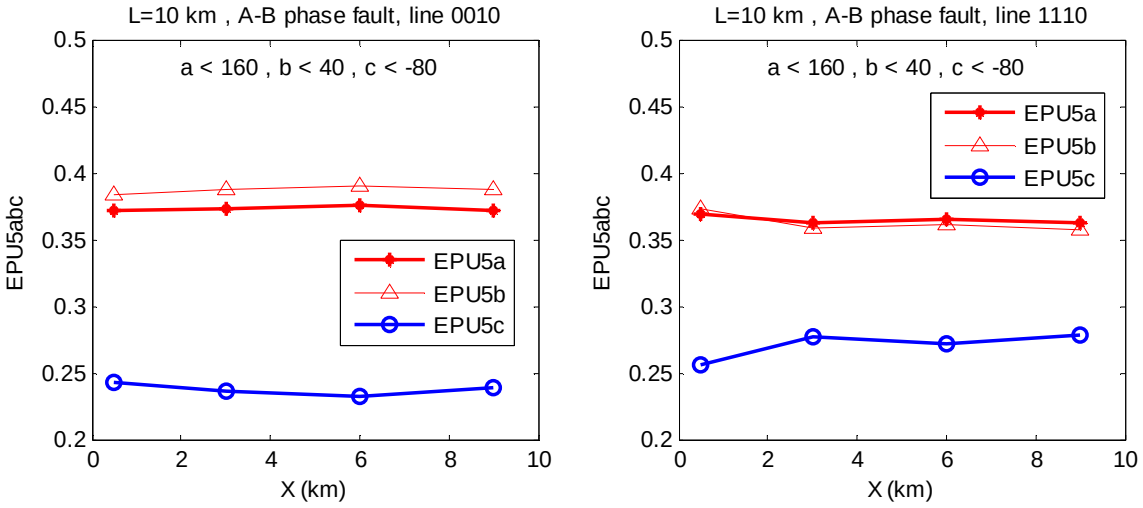

Figure 12. A-B two-phase fault.

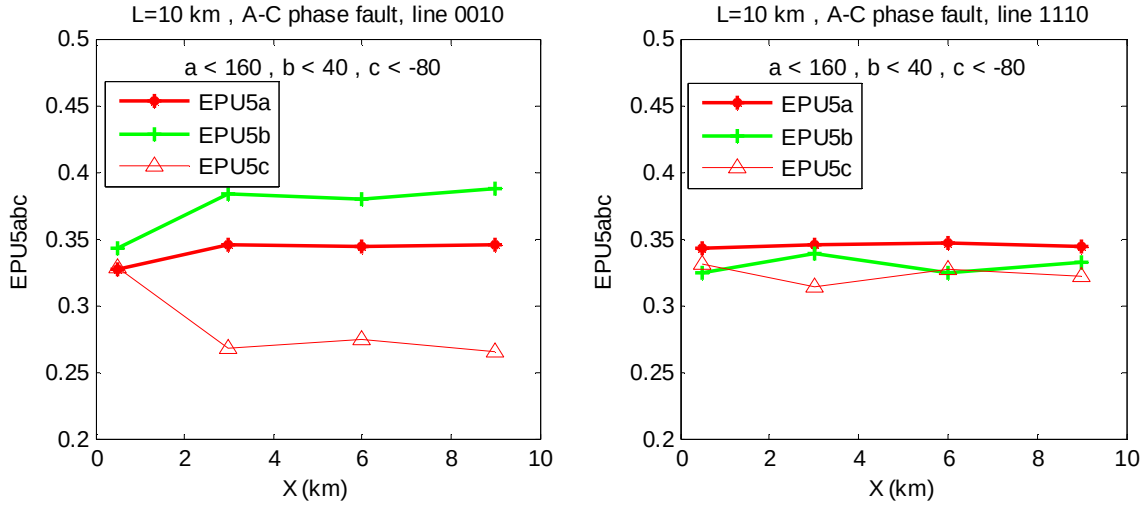

Figure 13. A-C two-phase fault.

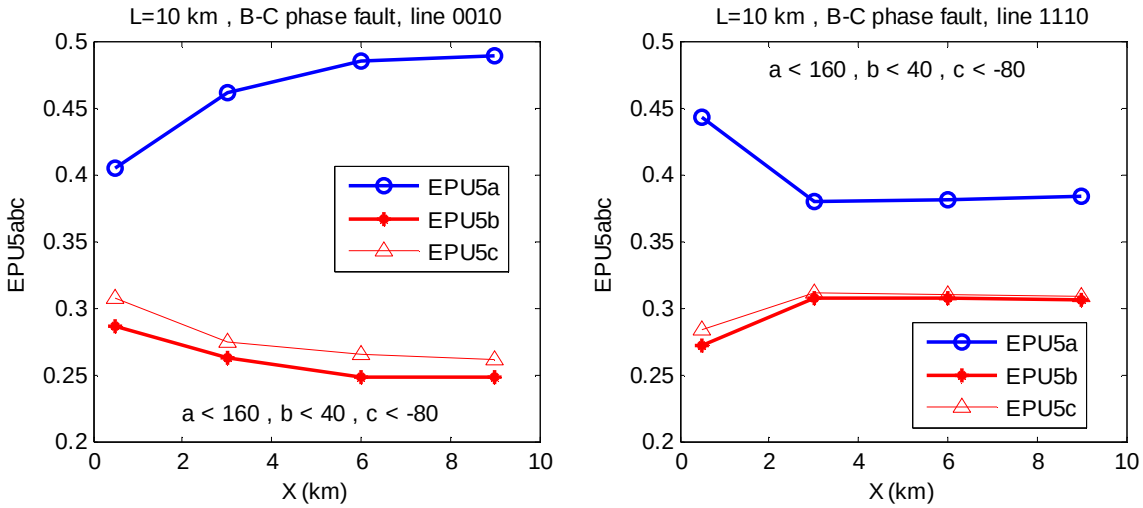

Figure 14. B-C two-phase fault.

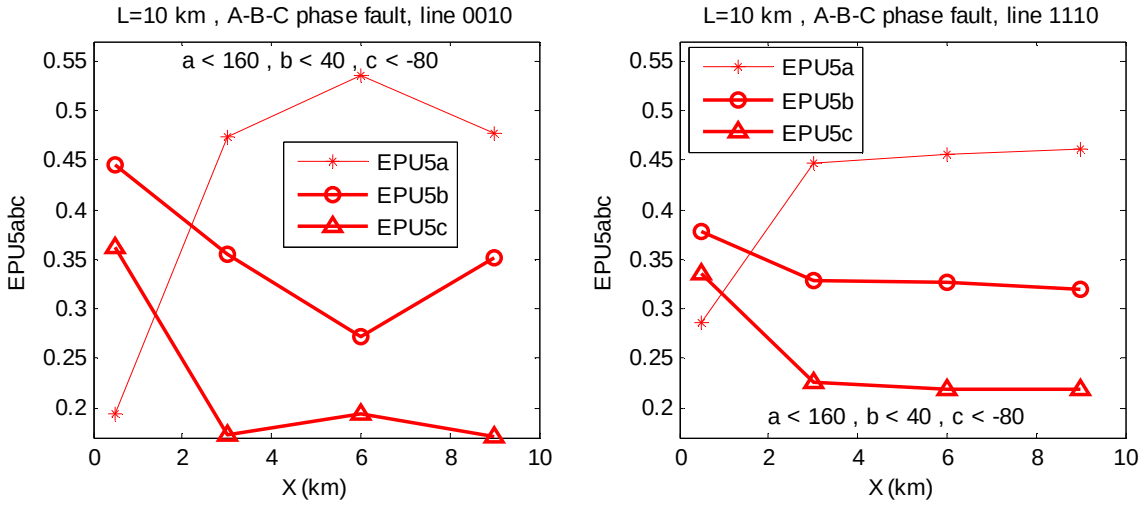

Figure 15. A-B-C three-phase fault.

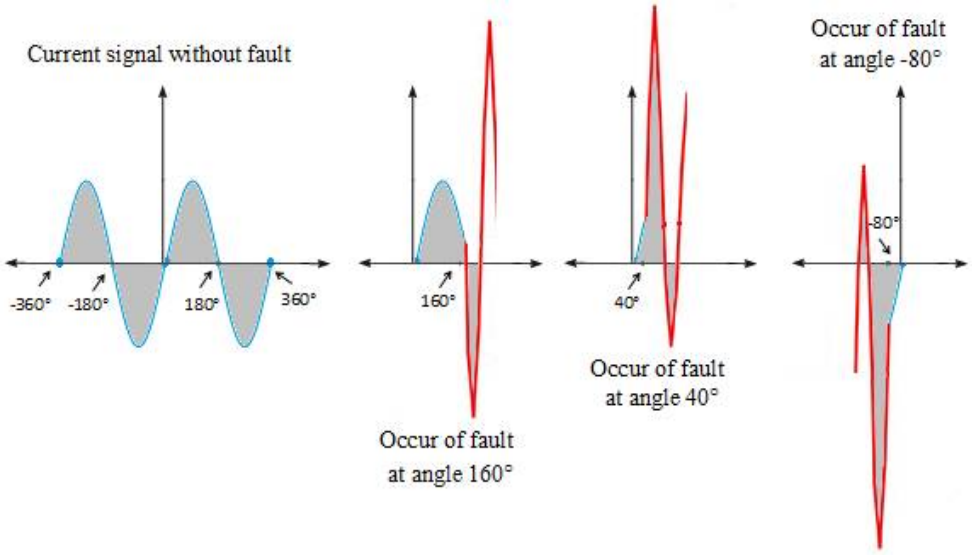

Figure 16. Area under curve current in normal conditions and in times of fault for angles of -80, 40, 160 degrees

Therefore, to generate the training data, the angle of occurrence of the fault should be considered and the range of the resistances should be selected properly to allow accurately providing the entropy variations for the neural network and allow the neural network to design a proper algorithm for fault location using transfer functions. Therefore, using the information in table 2, one could generate the training entropies and finally make a relationship between the input and output using the transfer function in figure 2 to train the neural network. In table 3, the number of entropies are shown for the training of the neural network for different faults.

The network could be tested after training the neural network. Table 4 and figure 17 show the estimated and actual values.

Also, one could calculate the error percentage of the estimation, using (17). According to the results, the estimation error percentage is shown in table 4 and figure 18.

$$\Re = \frac{|ActualLocation - EstimatedLocation|}{LengthofLine} \times 100 \quad (17)$$

Table 3. The number of entropies for the training of the neural network.

Fault type	Number of training data = $N_{line} \times N_{fault} \times N_{resistance} \times N_{location}$
ph.g 1	1088 = 4 × 6 × 3 × 14
ph.g 2	1088 = 4 × 6 × 3 × 14
Ph 2	168 = 4 × 3 × 14
Ph 3	56 = 4 × 14
Total	2400

Table 4. The results of testing the proposed design.

Actual values				Estimated values			RE (%)
Section	Fault type	Rf (ohm)	X (km)	Se	Rfe (ohm)	Xe (km)	
0001	A-g	0.5	5	0001	0.67	4.95	0.46
0010	A-B-g	7	4	0010	7.10	3.89	1.04
0011	A-B-C		7	0011		6.96	0.34
0100	B-g	25	7	0100	27.23	7.14	1.41
0101	C-g	35	3	0101	36.57	2.94	0.53
0110	B-C-g	45	0.6	0110	47.13	0.59	0.05
0111	A-B		6	0111		6.12	1.25
1000	A-C-g	65	3	1000	65.93	2.98	0.13
1001	A-B-C		2	1001		1.97	0.25
1010	C-g	85	8	1010	84.78	8.12	1.24
1011	A-g	95	7	1011	93.98	7.02	0.23
1100	B-g	10	4	1100	11.10	3.95	0.43
1101	A-B-g	75	2	1101	76.04	1.87	1.25
1110	B-C-g	55	5	1110	54.27	5.15	1.50
0011	A-C-g	100	4	0011	99.98	4.03	0.35
0111	B-g	14	9	0111	15.11	9.02	0.25
1001	A-B-g	2	6	1001	2.24	5.97	0.26
1011	B-C		2	1011		1.98	0.19
0110	A-C		8	0110		7.99	0.09

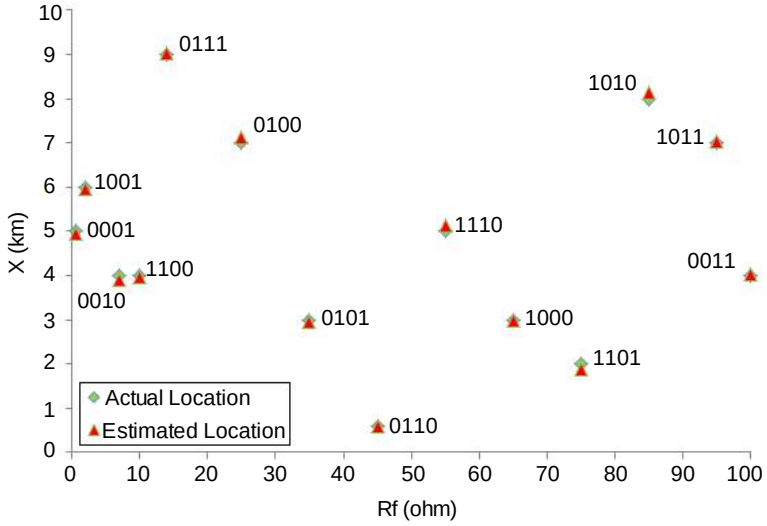

Figure 17. Comparison actual location and estimated location.

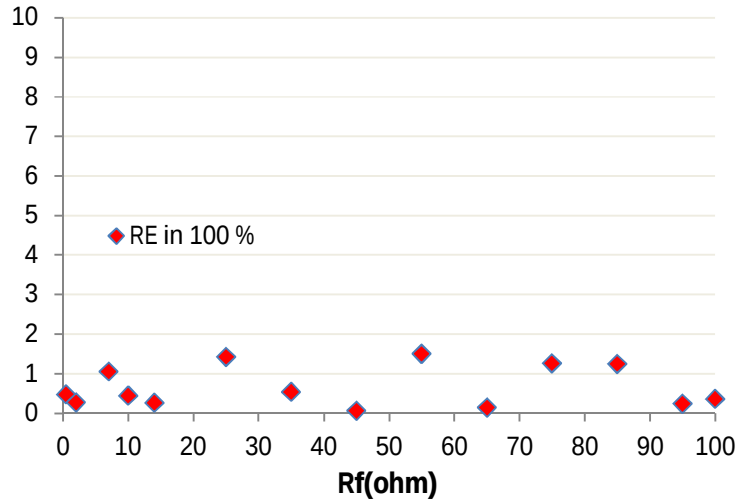

Figure 18. Estimation error percentage.

5. Review the results

In Figure 6, Figure 7 and Figure 8, the calculated entropy of the three-phase for the single-phase fault to ground is shown on the main line (0010) and the lateral branch (1110), respectively. Given the above mentioned, the entropy of the fault phase is a two-phase symmetric in this case. The reason of the difference between the entropy changes of line 0010 and 1110 is due to the fact that one of them is the main line and the other is the branch of the network, and the length of the network also causes a change in the line impedance, which also reduces entropy.

The calculated three-phase entropy is shown for a two-phase fault to the ground in Figure 9, Figure 10 and Figure 11. In this case, the entropy of the two phases is symmetric, however, they are not necessarily two phase faults due to the phase difference of 120 degrees between the phases a, b, and c and the presence of the lateral branch. Therefore, the symmetry in lines 0010 and 1110 will be different for two main reasons as explained below.

1. Main and lateral branches of line 0010, 1110

2. 120 degrees' phase difference with respect to each other

The entropy of the calculated three-phase for the two-phase fault is shown in Figure 12, Figure 13, and Figure 14. In this case, the entropy of the two-phase is symmetric, however these changes are not similar to the two-phase fault, since there is no ground resistance factor in this way, therefore, the exact effect of the fault resistance on the entropy changes will be evident.

The calculated entropy of the three-phase for the three-phase fault is shown in Figure 15. In this case, the two-phase entropy of each other is also symmetric. In Fig.16, the fault rate is shown at the angles of 160, 40 and 80 degrees. The question that arises is that if the fault occurs at a zero angle, is the design algorithm in trouble? The response is 'No', since the entropy variations may be negligible at zero degrees, whereas we have two other phases that have 120 degrees of phase difference with phase fault, and since we simultaneously compute the three-phase entropy, hence, our algorithm will not be affected. Meanwhile, if we want to calculate the fault at different angles, this entropy symmetry will not change due to the 120 degrees' phase difference with respect to each other.

1. Component level 5 is used in this paper. It should be noted that in the transformation of the wavelet, the higher the level of parsing on the signal, the more detailed components of the variation become accurate in the proposed algorithm of Level 5 than the 4th and 6th levels.

2. In most ANN designs, a neural network with a hidden layer is used. However, in this design, two neural networks were used, one to detect the area and the other to locate the fault in that section. Meanwhile, the hidden double layer is used. According to the results, we used two hidden layers due to the complexity of the entropy changes and the fact that we could well teach these changes to the neural network. Therefore, in this scheme, the fault field can be quickly obtained and then calculate the precise location of the fault. Hence, when the maximum fault in this algorithm is 1.5%, it means that there is 1.5% fault in that section, not in the entire network line, and since the length of each section is 10 km, the maximum fault is 150 m. Therefore, the accuracy of the fault finding in this scheme is high.

3. The aim of this paper is the simultaneous use of all three phases of the grid so that if the fault occurs at an angle of 0 degrees, we have two other phases, therefore, our algorithm is not compromised, and since the a, b, c phases are 120 degrees of angle difference, these entropy changes are well understood, and it solves the problem of fault at various angles.

Furthermore, the proposed scheme illustrates the effect of phase differences, as well as the fault resistance on computed entropies.

6. Conclusions

In this study, two neural networks are used for fault identification and location in the distribution network such that the training data are generated by wavelet transform of the fault signal observed by the relay and finally, calculating the three-phase currents entropy and positive and zero sequence energies. Also, the studies show that the entropies strongly depend on the fault occurrence angle, type of the fault and fault resistance. Therefore, the training data are purposefully selected to accurately introduce the fault characteristics to the neural network.

In this design, since the entropy varies for different fault resistances, the rate of the training samples are considered to be higher for to-ground faults compared to the phase-to-phase faults. Also, positive and zero sequences energies are used for the detection of fault and ground fault which is helpful in detecting the fault section. The simulation results show that the proposed algorithm is able to identify the fault location for high resistances. Also, the maximum estimation error in obtained to be 1.5%.

References

[1] A.A. Girgis, C.M. Fallon, D.L. Lubkeman. A fault location technique for rural distribution feeders. IEEE Transactions on Industry Applications. 29 (1993) 1170-5.

[2] G.D. Ferreira, D.d.S. Gazzana, A.S. Bretas, A.H. Ferreira, A.L. Bettiol, A. Carniato. Impedance-based fault location for overhead and underground distribution systems. North American Power Symposium (NAPS), 2012. IEEE2012. pp. 1-6.

[3] J.J. Mora-Flórez, R.A. Herrera-Orozco, A.F. Bedoya-Cadena. Fault location considering load uncertainty and distributed generation in power distribution systems. IET Generation, Transmission & Distribution. 9 (2015) 287-95.

[4] M. Saha, E. Rosolowski, J. Izykowski. Atp-emtp investigation for fault location in medium voltage networks. International Conference on Power Systems Trasients2005.

[5] H. Shodja, M. Khezri, A. Hashemian, A. Behzadan. RKPM with augmented corrected collocation method for treatment of material discontinuities. Computer Modeling in Engineering & Sciences(CMES). 62 (2010) 171-204.

[6] F. Nofeli, H. Arabshahi. Steady-state electron transport of wurtzite bulk ZnO. International Journal of Engineering Research and Applications (IJERA). 3 (2013) 2124-6.

[7] R.H. Salim, M. Resener, A.D. Filomena, K.R.C. De Oliveira, A.S. Bretas. Extended fault-location formulation for power distribution systems. IEEE transactions on power delivery. 24 (2009) 508-16.

[8] A.D. Filomena, M. Resener, R.H. Salim, A.S. Bretas. Fault location for underground distribution feeders: An extended impedance-based formulation with capacitive current compensation. International Journal of Electrical Power & Energy Systems. 31 (2009) 489-96.

[9] F.H. Magnago, A. Abur. A new fault location technique for radial distribution systems based on high frequency signals. Power Engineering Society Summer Meeting, 1999 IEEE. IEEE1999. pp. 426-31.

[10] D.W. Thomas, R.J. Carvalho, E.T. Pereira. Fault location in distribution systems based on traveling waves. Power Tech Conference Proceedings, 2003 IEEE Bologna. IEEE2003. p. 5 pp. Vol. 2.

[11] A. Borghetti, M. Bosetti, M. Di Silvestro, C.A. Nucci, M. Paolone. Continuous-wavelet transform for fault location in distribution power networks: Definition of mother wavelets inferred from fault originated transients. IEEE Transactions on Power Systems. 23 (2008) 380-8.

[12] R.H. Salim, K.R.C. de Oliveira, A.D. Filomena, M. Resener, A.S. Bretas. Hybrid fault diagnosis scheme implementation for power distribution systems automation. IEEE Transactions on Power Delivery. 23 (2008) 1846-56.

[13] M. Lotfi, M. Vidyasagar. A fast noniterative algorithm for compressive sensing using binary measurement matrices. IEEE Transactions on Signal Processing. (2018).

[14] A. Araghi, M. Pasebanpoor. Assessment of Pilot Pollution Problem for Multi-Cell Multi-User MIMO. Journal of Electrical and Electronic Engineering. 6 (2018) 120-8.

[15] U. Dwivedi, S. Singh, S. Srivastava. A wavelet based approach for classification and location of faults in distribution systems. India Conference, 2008 INDICON 2008 Annual IEEE. IEEE2008. pp. 488-93.

[16] W. Zhao, Y. Song, Y. Min. Wavelet analysis based scheme for fault detection and classification in underground power cable systems. Electric Power Systems Research. 53 (2000) 23-30.

[17] K.L. Butler-Purry, J. Cardoso. Characterization of underground cable incipient behavior using time-frequency multi-resolution analysis and artificial neural networks. Power and Energy Society General Meeting-Conversion and Delivery of Electrical Energy in the 21st Century, 2008 IEEE. IEEE2008. pp. 1-11.

[18] C. Teo. Automation of knowledge acquisition and representation for fault diagnosis in power distribution networks. Electric power systems research. 27 (1993) 183-9.

[19] E. Mohamed, N. Rao. Artificial neural network based fault diagnostic system for electric power distribution feeders. Electric Power Systems Research. 35 (1995) 1-10.

[20] D. Chan, C. Lu. Distribution system fault identification by mapping of characteristic vectors. Electric Power Systems Research. 57 (2001) 15-23.

[21] M.A. Al-shaher, M.M. Sabry, A.S. Saleh. Fault location in multi-ring distribution network using artificial neural network. Electric Power Systems Research. 64 (2003) 87-92.

[22] L.S. Martins, V.F. Pires, C. Alegria. A new accurate fault location method using αβ space vector algorithm. 14th PSCC (Power Systems Computation Conference)2002. pp. 1-6.

[23] J. Mora-Florez, J. Cormane-Angarita, G. Ordonez-Plata. K-means algorithm and mixture distributions for locating faults in power systems. Electric Power Systems Research. 79 (2009) 714-21.

[24] D. Thukaram, H. Khincha, H. Vijaynarasimha. Artificial neural network and support vector machine approach for locating faults in radial distribution systems. IEEE Transactions on Power Delivery. 20 (2005) 710-21.

[25] F. Chunju, K. Li, W. Chan, Y. Weiyong, Z. Zhaoning. Application of wavelet fuzzy neural network in locating single line to ground fault (SLG) in distribution lines. International Journal of Electrical Power & Energy Systems. 29 (2007) 497-503.

[26] M. Lotfi, B. Nazari, S. Sadri, N.K. Sichani. The detection of dacrocyte, schistocyte and elliptocyte cells in iron deficiency anemia. Pattern Recognition and Image Analysis (IPRIA), 2015 2nd International Conference on. IEEE2015. pp. 1-5.

[27] M. Lotfi, M. Vidyasagar. A fast single-pass algorithm for compressive sensing based on binary measurement matrices. Communication, Control, and Computing (Allerton), 2017 55th Annual Allerton Conference on. IEEE2017. pp. 369-73.

[28] P. Bhowmik, P. Purkait, K. Bhattacharya. A novel wavelet transform aided neural network based transmission line fault analysis method. International Journal of Electrical Power & Energy Systems. 31 (2009) 213-9.

[29] S. Hongchun, S. Xiangfei, S. Dajun. A new method for locating faults on transmission lines based on rough set and FNN. Power System Technology, 2002 Proceedings PowerCon 2002 International Conference on. IEEE2002. pp. 2584-8.

[30] J. Sadeh, H. Afradi. A new and accurate fault location algorithm for combined transmission lines using adaptive network-based fuzzy inference system. Electric Power Systems Research. 79 (2009) 1538-45.

[31] A.C. Adewole, R. Tzoneva, S. Behardien. Distribution network fault section identification and fault location using wavelet entropy and neural networks. Applied soft computing. 46 (2016) 296-306.

[32] S. Samantaray, B. Panigrahi, P. Dash. High impedance fault detection in power distribution networks using time–frequency transform and probabilistic neural network. IET generation, transmission & distribution. 2 (2008) 261-70.

[33] Z. He, L. Fu, S. Lin, Z. Bo. Fault detection and classification in EHV transmission line based on wavelet singular entropy. IEEE transactions on Power Delivery. 25 (2010) 2156-63.

[34] S. Ekici, S. Yildirim, M. Poyraz. Energy and entropy-based feature extraction for locating fault on transmission lines by using neural network and wavelet packet decomposition. Expert Systems with Applications. 34 (2008) 2937-44.